

## Contact line instability of a constant volume flow

J. M. Gomba,\* J. Diez,<sup>†</sup> R. Gratton,<sup>†</sup> and A.G. González<sup>†</sup>  
*Instituto de Física Arroyo Seco, Universidad Nacional del Centro  
 de la Provincia de Buenos Aires, Pinto 399, 7000, Tandil, Argentina*

L. Kondic<sup>‡</sup>

*Department of Mathematical Sciences and Center for Applied Mathematics and Statistics  
 New Jersey Institute of Technology, Newark, NJ 07102*

We study numerically the contact line stability of a constant volume (CV) of fluid spreading down an incline (see Fig. 1), as an example of a flow with no translational invariance. Within the lubrication approximation, we use a precursor film to relax the contact line singularity. Unlike the constant flux case, the base flow of the present situation depends on time. Consequently, we simultaneously solve the time evolution of the base flow and perturbations by means of a finite difference numerical code which uses an integral method developed here. The main difficulty lies in the fact that the base state is time-dependent, as it occurs in most of the flows found in applications. The analysis presented here avoids the use of simplified conditions, such as the imposition of a constant fluid thickness in the bulk region -constant flux (CF) flow-, and aims to give a more accurate description of the instability in realistic flows.

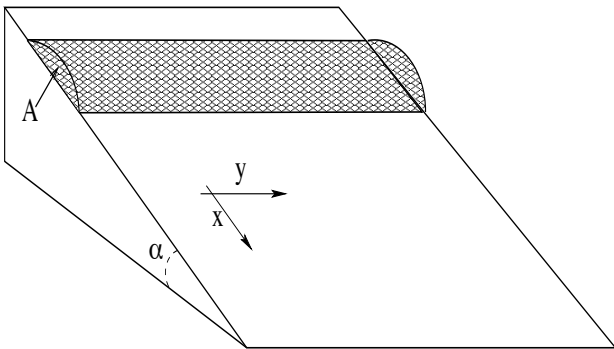


FIG. 1: Scheme of the inclined plane and coordinates axes.

One hindrance found when solving the linear equation that governs the evolution of the perturbations is that its coefficients depend on the flow velocity,  $v$ . Since  $v$  depends on a third order derivative of the thickness  $h$ , the requirement of high accuracy in the calculation implies the use of a relatively small grid size,  $\Delta x$ . Here, we develop an integral method to calculate  $v$  which yields a more accurate velocity profile in the front region than the standard finite difference scheme for a given  $\Delta x$ . One of the merits of this method is its simplicity and ease of adapting to other flow configurations.

For the CV flow, the perturbation travels with the same velocity as the front and, after a short transient

period, it adopts an asymptotic final shape. Regarding the amplitude of the perturbation, we find that our computations reproduce the linear growth reported in the experiments of Ref. [1].

The time evolution of both the power spectrum,  $g_m(\lambda, t)$ , and the growth rate,  $\sigma(\lambda, t)$ , shows some relevant features of the dynamics of the perturbation. For instance, the wavelength corresponding to the mode of maximum amplitude,  $\lambda_{max}$ , is time-dependent and decreases until an asymptotic value is reached, unlike the CF flow where it remains fixed. Moreover, we show that the instantaneous growth rate of  $\lambda_{max}$  is not necessarily largest at all times. This is possible since  $\sigma$  depends on time, and then, the amplitude of each mode for the CV flow is given by the time integral  $\exp[\int \sigma(t) dt]$ .

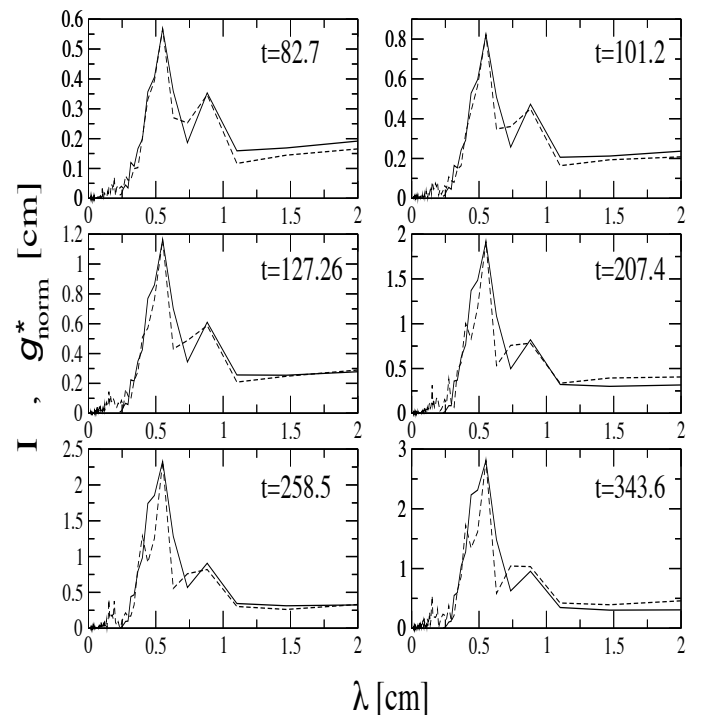


FIG. 2: Comparison between the experimental power spectra,  $I(t; \lambda)$ , (dashed line) and the normalized numerical power spectra,  $g_{norm}^*(t; \lambda)$ , (solid line).

When all modes have the same initial amplitude,  $\lambda_{max}$

is in good agreement with the experimental data for the films of silicon oil (PDMS) with capillary length  $a = 0.145 \text{ cm}$  on a vertical plane. In the typical case studied here, we estimate  $\lambda_{max} = 0.49 \text{ cm}$ , which is reasonably close to the experimental value,  $\lambda_{max}^{exp} = 0.55 \text{ cm}$ . The difference between these wavelengths is due to the fact that in experiments the initial amplitudes of the modes are not necessarily equal to each other, as we set in the simulations. The agreement between these wavelengths is complete when experimental amplitudes at an early time are used as inputs in the calculations (see Fig. 2).

The study of the dependence of the most unstable wavelength,  $\lambda_{max}$ , with the cross sectional area,  $A$ , confirms the power law dependence found in previous works for inclination angle  $\alpha = 90^\circ$  [2, 3]. Moreover, here we show that this dependence is still valid for  $\alpha \neq 90^\circ$ , with the same exponent. We also study the effect of  $\alpha$  on  $\lambda_{max}$  ( $5^\circ \leq \alpha \leq 90^\circ$ ), and conclude that a relationship of the type

$$\lambda_{max} \propto A^{0.27}/(\sin \alpha)^{0.247}, \quad (1)$$

holds for the range of  $A$ 's explored in this work, namely  $(4 \times 10^{-4}, 2 \times 10^{-3}) \text{ cm}^2$ . This dependence confirms the predictions in Ref. [3], but differs from those reported for much larger areas [4–6]. In fact, the fluid areas used in those experiments are  $\approx 1 - 10 \text{ cm}^2$ , that is  $10^3 - 10^4$  times the cross sections considered in this work, so that the capillary effects are small in those cases. As seen here, as well as in the literature [7–9], surface tension yields to the formation of a ridge in the front region, which is in turn responsible for the instability. For relatively thick films (i.e. for large Bond number  $B = (h_c/a)^2$ , where  $h_c$  is a characteristic thickness), the front region not only shows this ridge, but also adopts the shape of a caterpillar [10, 11]. Then, the spreading proceeds mainly due to the rolling motion at the head of the spreading and, consequently, the dynamics is qualitatively different for small and large  $B$ . Only when the average thickness becomes of the order of the capillary length,  $a$ , the shape of the front region changes from caterpillar to wedge [11]. This explains why the scaling laws for  $\lambda_{max}$  are different for small and large Bond numbers. Therefore, the cases studied here show that the spreading of small volumes of fluids constitutes an example where the knowledge of large scale physics cannot be directly applied to micro-metrics flows.

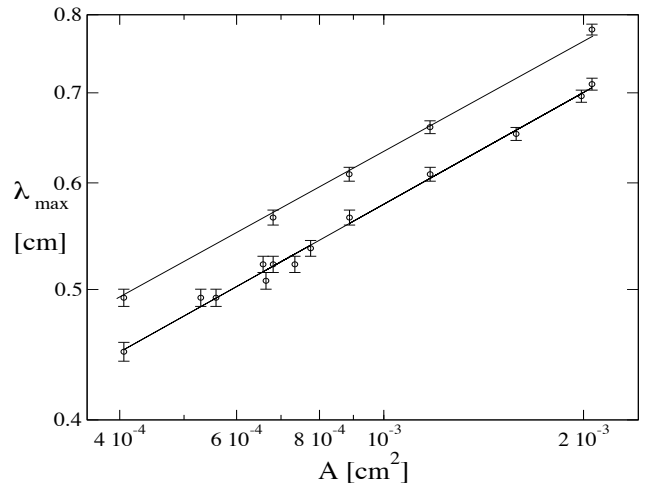


FIG. 3: Dependence of the most unstable mode,  $\lambda_{max}$ , with the cross section,  $A$ , for  $\alpha = 45^\circ$  (upper set of points) and  $\alpha = 90^\circ$  (lower set of points).

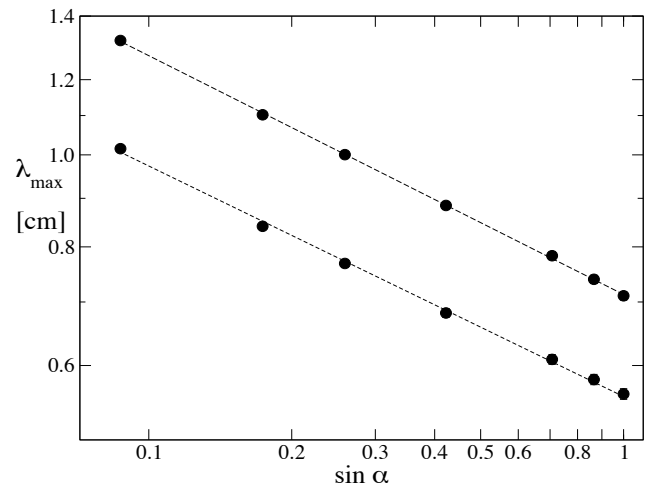


FIG. 4: Dependence of  $\lambda_{max}$  on the inclination angle,  $\alpha$ , for  $A = 1.97 \times 10^{-3} \text{ cm}^2$  (upper set of points) and  $A = 9 \times 10^{-4} \text{ cm}^2$  (lower set of points).

\* CONICET, Argentina.; Electronic address: jgomba@exa.unicen.edu.ar

† CONICET, Argentina.

‡ URL: <http://m.njit.edu/~kondic>

[1] A. G. González, J. Diez, J. Gomba, R. Gratton, and L. Kondic, Phys. Rev. E **70**, 026309 (2004).

[2] L. W. Schwartz, Phys. Fluids A **1**, 443 (1989).

[3] J. Gomba, J. Diez, A. G. González, and R. Gratton, Phys. Rev. E **71**, 016304 (2005).

[4] H. Huppert, Nature **300**, 427 (1982).

[5] J. M. Jerrett and J. R. de Bruyn, Phys. Fluids A **4**, 234 (1992).

[6] Y. Ye and H. Chang, Phys. Fluids **11**, 2494 (1999).

[7] S. M. Troian, E. Herbolzheimer, S. A. Safran, and J. F. Joanny, Europhys. Lett. **10**, 25 (1989).

[8] L. M. Hocking and M. J. Miksis, J. Fluid. Mech. **247**, 157 (1993).

[9] A. L. Bertozzi and M. P. Brenner, Phys. Fluids **9**, 530 (1997).

[10] H.-C. C. I. Veretennikov, A. Indeikina, J. Fluid. Mech. **373**, 81 (1998).

[11] B. M. Marino, L. P. Thomas, J. A. Diez, and R. Gratton, J. Colloid Interface Sci. **177** (1996).